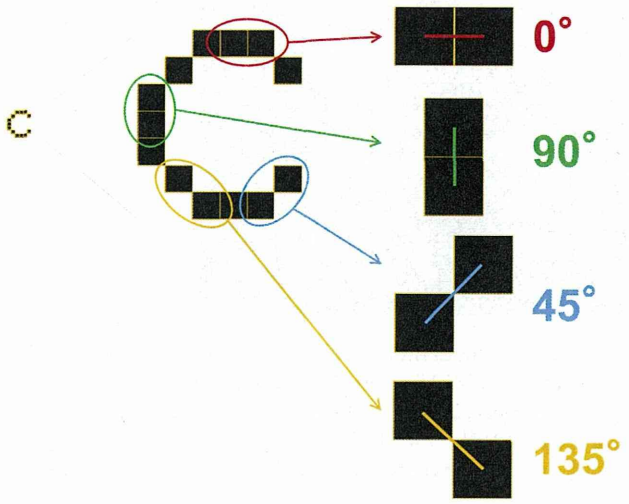

FIGURE 2. Example of calculation of parallelism. A digital representation of the letter "C," which consists of 13 pixels, is used for calculation of parallelism. In digital images, pixels are adjoined to each other in 45-degree increments in 8 different directions and angles of a neighboring pixel pair can be categorized as 0 (red), 45 (blue), 90 (green), and 135 degrees (yellow) against the horizon. In this study, parallelism is calculated as follows: Parallelism = $(|n_0 - n_{90}| + |n_{45} - n_{135}|)/(n_0 + n_{45} + n_{90} + n_{135})$, where n_0, n_{45}, n_{90}, and n_{135} are the numbers of pixel pairs at 0, 45, 90, and 135 degrees, respectively. Parallelism can range from 0-1 and increases as the retinal layers run more parallel with each other. In analysis of a curved segment, parallelism is equivalent to the ratio of straight-line distance between the starting point and end point to the whole length of the curved segments. However, in this study, parallelism is designed to count discretization of the angle in 45-degree increments in the case of multiple line segments in the image, which is not in strict accordance with the above-mentioned definition. In the example, $n_0 = 4$, $n_{45} = 3$, $n_{90} = 2$, and $n_{135} = 3$, and parallelism = 0.167.

• CALCULATION OF PARALLELISM: To quantitatively evaluate orientations of retinal layers, we first extracted skeletonized images (line art) from OCT images by applying filtration through first-order derivative of a Gaussian filter using the ImageJ plug-in Feature Detector, an algorithm based on the optimization of a Canny-like criterion,[28–31] followed by a 1-2 pixel band-pass filter and binarization by intensity thresholding using Otsu's thresholding method for automatic binarization level decision (Figure 1).[25,26,32] Because the target object of image processing in this study was a 6-mm-long section on a full-thickness OCT image, filter bandwidth was adjusted to reduce noise in the images with maintenance of visualization of multiple layers. Lines in the vitreous space and beyond the retinal pigment epithelium were erased manually as artifacts. ERMs were not erased and were included in analyses. Note that the analysis requires only information regarding layer orientation, which can be obtained using line segments, and not solid lines or accurate segmentation of the retinal layers.

In the skeletonized images, angles of neighboring pixel pairs against the horizon were categorized as 0, 45, 90, and 135 degrees, and the numbers of pixel pairs were counted, basically according to the study by Ueda and associates on actin filament-bundle orientations in plants (Figure 2).[26] In this study, "Parallelism" referred to the orientations of retinal layers and was calculated using the ImageJ plug-in KbiLinesAngle (http://hasezawa.ib.k.u-tokyo.ac.jp/zp/Kbi/ImageJKbiPlugins), as follows:

$$\text{Parallelism} = (|n_0 - n_{90}| + |n_{45} - n_{135}|)/(n_0 + n_{45} + n_{90} + n_{135})$$

where n_0, n_{45}, n_{90}, and n_{135} are the numbers of pixel pairs orientated at 0, 45, 90, and 135 degrees, respectively.[25,26] Parallelism ranges from 0-1 and increases as the retinal layers run more parallel with each other. All digital images were processed by a single operator (A.U.) using ImageJ (developed by Wayne Rasband, National Institutes of Health, Bethesda, Maryland, USA; available at http://rsb.info.nih.gov/ij/index.html) and its plug-in software.

Parallelism was calculated in an area 6 mm in length centered on the fovea and in the following 5 subfields: center (1 mm), 2 parafovea (0.5-1.5 mm), and 2 perifovea (1.5-3.0 mm) (Figure 3). Furthermore, in each subfield, parallelism was calculated in the area above the outer nuclear layer (ONL) space as the inner layer and in the area below the ONL space as the outer layer.[33]

• STATISTICAL ANALYSIS: All values are expressed as the mean ± standard deviation. All BCVA measurements were converted to logarithm of the minimal angle of resolution (logMAR) equivalents before statistical analysis. Student *t* tests were used to compare the 2 groups (normal subjects vs ERM patients) regarding age, logMAR VA, parallelism, and retinal thickness. Comparisons of parallelism and retinal thickness of the 5 subfields were carried out using repeated-measures analysis of variance, and differences between the 2 groups were analyzed using the paired *t* test followed by Bonferroni correction. Associations of metamorphopsia scores with parallelism and retinal thickness and of logMAR VA with parallelism and retinal thickness were analyzed using the Pearson correlation coefficient. Stepwise regression analysis was performed to evaluate the contribution made by parallelism and retinal thickness of the 5 subfields to the horizontal metamorphopsia score, vertical metamorphopsia score, and logMAR VA. Furthermore, correlation between parallelism and retinal thickness was analyzed using the Pearson correlation coefficient. A *P* value of $<.05$ was considered statistically significant. All analyses, except for multiple linear regression analysis, were performed using StatView (version 5.0; SAS Institute, Cary, North Carolina, USA). Stepwise regression analysis was performed using SPSS (Version 17; GraphPad Software, La Jolla, California, USA).

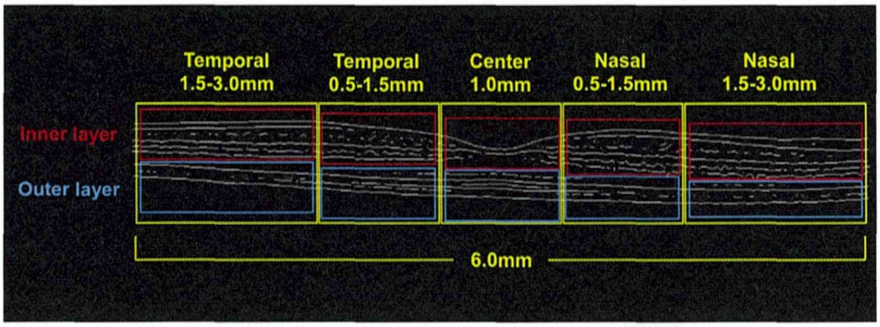

FIGURE 3. Regions of interest in skeletonized retinal layers in horizontal line scan of optical coherence tomographic image. Parallelism was calculated in a 6-mm-long area centered on the fovea and also in the 5 subfields: center (1 mm), 2 parafovea (temporal and nasal, 0.5-1.5 mm), and 2 perifovea (temporal and nasal, 1.5-3.0 mm). Furthermore, in each subfield, parallelism was calculated in the area above the outer nuclear layer (ONL) space as the inner layer and the area below the ONL space as the outer layer. Regions of interest in the skeletonized vertical line scan were similarly set on the image as follows: center (1 mm), 2 parafovea (inferior and superior, 0.5-1.5 mm), and 2 perifovea (inferior and superior, 1.5-3.0 mm).

RESULTS

SIX HORIZONTAL AND 7 VERTICAL SCANS OUT OF 57 SCAN pairs of ERM patients were excluded from the analyses because the central fovea could not be identified. A pair of horizontal and vertical scans in an ERM patient was also excluded from the analyses because of low image quality. Finally, skeletonized images were successfully obtained from the remaining 50 horizontal scans and 49 vertical scans of ERM patients and the 30 scan pairs of volunteers through semi-automatic image processing (Figures 1 and 4).

• PARALLELISM IN NORMAL SUBJECTS: Parallelism of normal subjects is shown in Table 1. In the horizontal scan, there were significant differences in full-thickness parallelism ($P = .0090$) and in inner-layer parallelism ($P < .0001$) among 5 subfields; however, significant differences were not shown in outer-layer parallelism among 5 subfields ($P = .0966$) (Supplemental Figure 1, available at AJO.com). In the vertical scan, significant differences were disclosed in full-thickness, inner-layer, and outer-layer parallelism values. Compared with the horizontal scan, parallelism of the perifovea (1.5-3.0 mm) tended to be lower than that of other subfields, and significant differences in full-thickness and outer-layer parallelism values were observed between the perifovea and some of the other subfields (Supplemental Figure 2, available at AJO.com). Vessel shadows were imaged as lines perpendicular to the retinal layers in skeletonized vertical scans, which might have decreased parallelism in the perifovea (Supplemental Figure 3, available at AJO.com). Retinal thickness was smallest in the center (1 mm) and greatest in the parafovea (0.5-1.5 mm) both in horizontal and in vertical scans.

• DIFFERENCES IN PARALLELISM BETWEEN NORMAL SUBJECTS AND PATIENTS WITH EPIRETINAL MEMBRANE: In many cases of ERM, line segments around the fovea were depicted in random directions, which probably contributed to decreased parallelism (Figure 4). Significant differences were observed in full-thickness parallelism between normal eyes and eyes with ERM except for the perifovea (inferior, 1.5-3.0 mm) in the vertical scan (Table 1). In the inner layer, parallelism was significantly lower in eyes with ERM than in normal eyes. In the outer layer, no significant differences were noted between the groups except for parallelism of the center (1 mm) in both the horizontal and vertical scans and parallelism of the perifovea (superior, 1.5-3.0 mm) in the vertical scan. Retinal thicknesses were significantly higher in eyes with ERM than in normal eyes.

• CORRELATION BETWEEN VISUAL FUNCTION AND PARALLELISM IN PATIENTS WITH EPIRETINAL MEMBRANE: In the horizontal scan, parallelism in the areas excluding the perifovea (nasal, 1.5-3.0 mm) correlated significantly with visual acuity and horizontal metamorphopsia score (Table 2). In particular, parallelism of the center (1 mm) had a strong correlation with horizontal metamorphopsia score ($R = -0.632$; $P < .0001$). Significant correlations were also found in all 5 subfields between parallelism and vertical metamorphopsia score. In the individual analysis of inner and outer layers, parallelism significantly correlated with horizontal and vertical metamorphopsia scores.

In the vertical scan, parallelism in the areas excluding the perifovea (inferior, 1.5-3.0 mm) was also significantly correlated with visual acuity and horizontal metamorphopsia score. Furthermore, parallelism had a correlation with vertical metamorphopsia score. Inner-layer parallelism correlated significantly with visual acuity, horizontal metamorphopsia score, and vertical metamorphopsia score in some of the subfields including the center (1 mm), while outer-layer parallelism showed a significant correlation between some of the subfields excluding the center (1 mm) and metamorphopsia score or visual acuity.

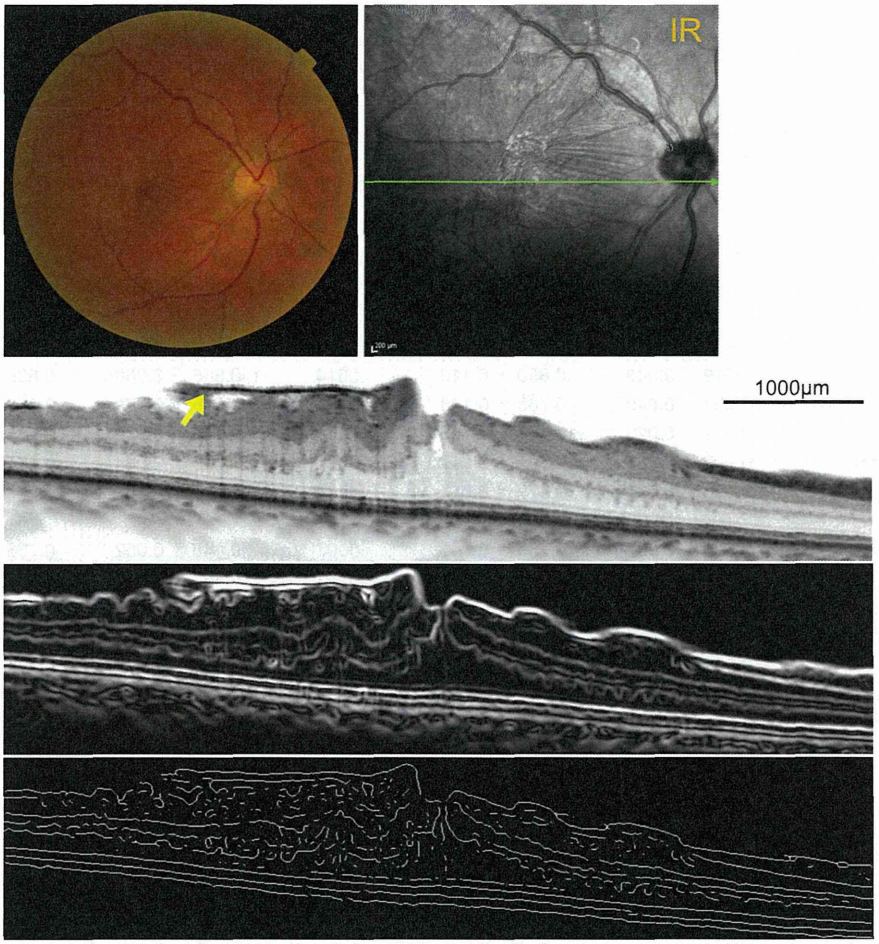

FIGURE 4. Extraction of skeletonized image from retinal layers in optical coherence tomographic images of patient with epiretinal membrane (ERM). Images of the right eye of a 55-year-old man with an idiopathic ERM. Snellen equivalent best-corrected visual acuity was 20/20 in this eye, and M-CHARTS metamorphopsia scores were 0.8 for horizontal lines and 1.1 for vertical lines. (Top left) Color fundus photograph shows retinal folds and irregular reflex in the fovea. (Top right) Infrared (IR) image clearly shows retinal folds, irregular reflex, and distortion of retinal vessels. (Second row) Spectral-domain optical coherence tomography (SDOCT) image of 6-mm-long section cropped from the horizontal line scan of the SDOCT image through the fovea in the direction of the horizontal arrow in top right panel shows the ERM (arrow) and distortions of retinal layers. (Third row) Filtered image of second row after application of derivative of a Gaussian filter for edge detection. (Bottom row) Skeletonized SDOCT image generated from third row. Segmented lines that are aligned randomly represent distorted layers in the original OCT image and are used to calculate parallelism. Parallelism calculated for the 6-mm section, full thickness of the center (1 mm), inner layer of the center (1 mm), and outer layer of the center (1 mm) was 0.833, 0.655, 0.344, and 0.947, respectively.

• CORRELATION BETWEEN VISUAL FUNCTION AND RETINAL THICKNESS IN PATIENTS WITH EPIRETINAL MEMBRANE: Retinal thickness correlated significantly with visual acuity and vertical and horizontal metamorphopsia scores in some of the subfields, including the center (1 mm) in both horizontal and vertical scans (Table 2).

• CORRELATION BETWEEN PARALLELISM AND RETINAL THICKNESS IN PATIENTS WITH EPIRETINAL MEMBRANE: Significant negative correlations were found between full-thickness and inner-layer parallelism and retinal thickness in all subfields of horizontal and vertical scans (Table 3). Multiple significant correlations were also found between outer-layer parallelism and retinal thickness in some of the subfields of horizontal and vertical scans.

• MULTIVARIATE ANALYSIS: Analysis included 10 independent variables (full-thickness parallelism in 5 subfields and retinal thickness in 5 subfields).

In the horizontal scan, significant associations were found between parallelism of the center (1 mm) and horizontal metamorphopsia score ($\beta = -0.632$, $P < .001$), vertical metamorphopsia score ($\beta = -0.487$, $P < .001$), and visual acuity ($\beta = -0.522$, $P < .001$).

In the vertical scan, parallelism of the parafovea (inferior, 0.5-1.5 mm) correlated with horizontal

TABLE 1. Differences in Parallelism of Retinal Layers in Optical Coherence Tomographic Images Between Normal Subjects and Patients With Epiretinal Membrane

Characteristic	Horizontal Scan			Vertical Scan		
	Normal Eyes	Eyes With ERM	*P* Value	Normal Eyes	Eyes With ERM	*P* Value
No. eyes/patients	30/30	50/50	-	30/30	49/49	-
Men/women	18/12	24/26	-	18/12	24/25	-
Age (y)	64.5 ± 10.7	67.8 ± 7.5	.1141	64.5 ± 10.7	68.4 ± 7.2	.0549
Visual acuity (logMAR)	−0.150 ± 0.044	0.172 ± 0.206	<.0001	−0.150 ± 0.044	0.174 ± 0.205	<.0001
Parallelism full thickness						
6 mm	0.896 ± 0.034	0.800 ± 0.101	<.0001	0.857 ± 0.035	0.766 ± 0.093	<.0001
T or I, 1.5-3.0 mm	0.919 ± 0.043	0.850 ± 0.110	.0014	0.866 ± 0.060	0.839 ± 0.092	.1570
T or I, 0.5-1.5 mm	0.902 ± 0.040	0.765 ± 0.148	<.0001	0.875 ± 0.054	0.759 ± 0.119	<.0001
Center, 1.0 mm	0.922 ± 0.022	0.761 ± 0.135	<.0001	0.900 ± 0.029	0.735 ± 0.141	<.0001
N or S, 0.5-1.5 mm	0.903 ± 0.036	0.791 ± 0.117	<.0001	0.883 ± 0.054	0.736 ± 0.138	<.0001
N or S, 1.5-3.0 mm	0.908 ± 0.036	0.879 ± 0.062	.0208	0.862 ± 0.061	0.816 ± 0.116	.0466
Parallelism inner layer						
T or I, 1.5-3.0 mm	0.891 ± 0.057	0.789 ± 0.141	.0003	0.848 ± 0.052	0.798 ± 0.097	.0105
T or I, 0.5-1.5 mm	0.856 ± 0.063	0.667 ± 0.195	<.0001	0.840 ± 0.050	0.687 ± 0.144	<.0001
Center, 1.0 mm	0.839 ± 0.048	0.619 ± 0.185	<.0001	0.804 ± 0.056	0.592 ± 0.194	<.0001
N or S, 0.5-1.5 mm	0.867 ± 0.052	0.714 ± 0.154	<.0001	0.850 ± 0.057	0.658 ± 0.167	<.0001
N or S, 1.5-3.0 mm	0.897 ± 0.037	0.854 ± 0.071	.0029	0.852 ± 0.053	0.778 ± 0.130	.0038
Parallelism outer layer						
T or I, 1.5-3.0 mm	0.958 ± 0.044	0.963 ± 0.037	.5906	0.903 ± 0.072	0.930 ± 0.075	.1269
T or I, 0.5-1.5 mm	0.964 ± 0.023	0.953 ± 0.037	.1692	0.940 ± 0.046	0.932 ± 0.051	.4590
Center, 1.0 mm	0.965 ± 0.017	0.939 ± 0.043	.0024	0.956 ± 0.022	0.942 ± 0.030	.0343
N or S, 0.5-1.5 mm	0.959 ± 0.025	0.946 ± 0.032	.0541	0.949 ± 0.034	0.927 ± 0.059	.0788
N or S, 1.5-3.0 mm	0.947 ± 0.038	0.957 ± 0.031	.2093	0.887 ± 0.082	0.939 ± 0.047	.0006
Retinal thickness						
T or I, 1.5-3.0 mm	281 ± 14	338 ± 49	<.0001	283 ± 11	310 ± 42	<.0001
T or I, 0.5-1.5 mm	320 ± 13	430 ± 59	<.0001	338 ± 11	418 ± 55	<.0001
Center, 1.0 mm	251 ± 16	457 ± 82	<.0001	257 ± 19	454 ± 80	<.0001
N or S, 0.5-1.5 mm	337 ± 12	435 ± 60	<.0001	343 ± 12	427 ± 68	<.0001
N or S, 1.5-3.0 mm	315 ± 13	353 ± 49	<.0001	301 ± 13	344 ± 47	.0001

ERM = epiretinal membrane; I = inferior; LogMAR = logarithm of minimal angle of resolution; N = nasal; S = superior; T = temporal.

metamorphopsia score (ß = −0.465, $P = .001$) and vertical metamorphopsia score (ß = −0.524, $P < .001$). Visual acuity correlated with retinal thickness of the center (1 mm) (ß = 0.486, $P = .001$).

DISCUSSION

THE AIM OF THIS STUDY WAS TO FIND A NEW ROBUST AND practical surrogate marker, other than retinal thickness, for evaluation of retinal layer integrity. Study results demonstrated that "Parallelism," a parameter reflecting layer orientation, could be obtained using line segments in skeletonized OCT images and was clinically relevant in eyes with ERM. To the best of our knowledge, this is the first study that employed layer orientation in OCT image analysis.

In normal eyes, full-thickness parallelism, unlike retinal thickness, was nearly homogeneous, with slight variations according to location. Meanwhile, inner-layer parallelism had the smallest value in the center (1 mm) and outer-layer parallelism underwent very little change except at the perifovea (1.5-3.0 mm), where values were extremely small in the vertical scan, which might have been caused by vessel shadows imaged as lines perpendicular to the retinal layers. These results are thought to be attributable to the existence of the fovea at which the inner layers converge. Because vertical OCT scans include relatively large vessels in the areas of the perifovea (1.5-3.0 mm), which are not visualized in horizontal OCT scans, we suggest excluding these areas in the analysis of parallelism to remove artifacts.

Significant differences between normal eyes and eyes with ERM, and significant correlations with visual function, were detected in both parallelism and retinal thickness. Moreover, parallelism was strongly correlated with retinal thickness in ERM patients, suggesting that parallelism was comparative to retinal thickness in evaluation

TABLE 2. Correlation Between Visual Function and Parallelism of Retinal Layers in Optical Coherence Tomographic Images in Patients With Epiretinal Membrane

	Horizontal Scan			Vertical Scan		
	M-CHARTS Horizontal Metamorphopsia Score	M-CHARTS Vertical Metamorphopsia Score	Visual Acuity (LogMAR)	M-CHARTS Horizontal Metamorphopsia Score	M-CHARTS Vertical Metamorphopsia Score	Visual Acuity (LogMAR)
Parallelism full thickness						
6 mm	$P < .0001$; $R = -0.543$	$P = .0003$; $R = -0.482$	$P = .0016$; $R = -0.434$	$P = .0012$; $R = -0.453$	$P < .0001$; $R = -0.533$	$P = .0024$; $R = -0.428$
T or I, 1.5-3.0 mm	$P = .0063$; $R = -0.383$	$P = .0052$; $R = -0.391$	$P = .0257$; $R = -0.318$	$P = .1487$; $R = -0.214$	$P = .0012$; $R = -0.453$	$P = .4462$; $R = -0.114$
T or I, 0.5-1.5 mm	$P = .0002$; $R = -0.499$	$P = .0023$; $R = -0.421$	$P = .0050$; $R = -0.392$	$P = .0008$; $R = -0.465$	$P = .0001$; $R = -0.524$	$P = .0064$; $R = -0.389$
Center, 1.0 mm	$P < .0001$; $R = -0.632$	$P = .0003$; $R = -0.487$	$P < .0001$; $R = -0.522$	$P = .0035$; $R = -0.414$	$P = .0009$; $R = -0.462$	$P = .0018$; $R = -0.439$
N or S, 0.5-1.5 mm	$P = .0036$; $R = -0.404$	$P = .0220$; $R = -0.325$	$P = .0206$; $R = -0.329$	$P = .0074$; $R = -0.383$	$P = .0024$; $R = -0.428$	$P = .0292$; $R = -0.317$
N or S, 1.5-3.0 mm	$P = .1106$; $R = -0.231$	$P = .0148$; $R = -0.345$	$P = .0738$; $R = -0.258$	$P = .0184$; $R = -0.341$	$P = .0250$; $R = -0.326$	$P = .0061$; $R = -0.392$
Parallelism inner layer						
T or I, 1.5-3.0 mm	$P = .0052$; $R = -0.391$	$P = .0022$; $R = -0.422$	$P = .0445$; $R = -0.288$	$P = .0764$; $R = -0.261$	$P = .0026$; $R = -0.425$	$P = .4522$; $R = -0.113$
T or I, 0.5-1.5 mm	$P = .0004$; $R = -0.483$	$P = .0070$; $R = -0.378$	$P = .0139$; $R = -0.348$	$P = .0017$; $R = -0.440$	$P = .0007$; $R = -0.469$	$P = .0132$; $R = -0.357$
Center, 1.0 mm	$P < .0001$; $R = -0.621$	$P = .0034$; $R = -0.407$	$P = .0006$; $R = -0.466$	$P = .0040$; $R = -0.409$	$P = .0038$; $R = -0.410$	$P = .0077$; $R = -0.381$
N or S, 0.5-1.5 mm	$P = .0016$; $R = -0.435$	$P = .0255$; $R = -0.318$	$P = .0233$; $R = -0.322$	$P = .0163$; $R = -0.347$	$P = .0103$; $R = -0.369$	$P = .0581$; $R = -0.278$
N or S, 1.5-3.0 mm	$P = .0370$; $R = -0.298$	$P = .0570$; $R = -0.273$	$P = .0348$; $R = -0.302$	$P = .0131$; $R = -0.357$	$P = .0434$; $R = -0.295$	$P = .0071$; $R = -0.385$
Parallelism outer layer						
T or I, 1.5-3.0 mm	$P = .2754$; $R = -0.159$	$P = .0098$; $R = -0.363$	$P = .0388$; $R = -0.296$	$P = .4314$; $R = -0.118$	$P = .0421$; $R = -0.297$	$P = .9934$; $R = 0.001$
T or I, 0.5-1.5 mm	$P = .0568$; $R = -0.274$	$P = .0161$; $R = -0.341$	$P = .0198$; $R = -0.331$	$P = .0386$; $R = -0.302$	$P = .0010$; $R = -0.460$	$P = .0313$; $R = -0.314$
Center, 1.0 mm	$P = .0232$; $R = -0.323$	$P = .0160$; $R = -0.341$	$P = .0345$; $R = -0.302$	$P = .4311$; $R = -0.118$	$P = .5334$; $R = -0.094$	$P = .0700$; $R = -0.267$
N or S, 0.5-1.5 mm	$P = .3061$; $R = -0.150$	$P = .4339$; $R = -0.115$	$P = .3828$; $R = -0.128$	$P = .0470$; $R = -0.291$	$P = .0097$; $R = -0.371$	$P = .3365$; $R = -0.144$
N or S, 1.5-3.0 mm	$P = .7090$; $R = -0.055$	$P = .8746$; $R = 0.023$	$P = .6622$; $R = -0.064$	$P = .4689$; $R = 0.109$	$P = .8523$; $R = 0.028$	$P = .4219$; $R = 0.120$
Retinal thickness						
T or I, 1.5-3.0 mm	$P = .1261$; $R = 0.222$	$P = .2462$; $R = 0.169$	$P = .1106$; $R = 0.231$	$P = .3699$; $R = 0.134$	$P = .2903$; $R = 0.158$	$P = .0581$; $R = 0.278$
T or I, 0.5-1.5 mm	$P = .0009$; $R = 0.454$	$P = .0027$; $R = 0.416$	$P = .0059$; $R = 0.385$	$P = .0201$; $R = 0.337$	$P = .0076$; $R = 0.382$	$P = .0007$; $R = 0.472$
Center, 1.0 mm	$P = .0031$; $R = 0.410$	$P = .0078$; $R = 0.373$	$P = .0011$; $R = 0.447$	$P = .0018$; $R = 0.438$	$P = .0218$; $R = 0.333$	$P = .0004$; $R = 0.486$
N or S, 0.5-1.5 mm	$P = .1626$; $R = 0.203$	$P = .1231$; $R = 0.223$	$P = .0137$; $R = 0.348$	$P = .2168$; $R = 0.184$	$P = .2289$; $R = 0.179$	$P = .0026$; $R = 0.426$
N or S, 1.5-3.0 mm	$P = .2910$; $R = 0.154$	$P = .5059$; $R = 0.098$	$P = .1166$; $R = 0.227$	$P = .2663$; $R = 0.166$	$P = .2208$; $R = 0.183$	$P = .0034$; $R = 0.415$

ERM = epiretinal membrane; I = inferior; LogMAR = logarithm of minimal angle of resolution; N = nasal; S = superior; T = temporal.

TABLE 3. Correlation Between Parallelism of Retinal Layers and Retinal Thickness in Optical Coherence Tomographic Images of Patients With Epiretinal Membrane

	Parallelism		
	Full Thickness	Inner Layers	Outer Layers
Retinal thickness, horizontal scan			
Temporal, 1.5-3.0 mm	$P < .0001$; $R = -0.608$	$P < .0001$; $R = -0.614$	$P = .0138$; $R = -0.348$
Temporal, 0.5-1.5 mm	$P < .0001$; $R = -0.720$	$P < .0001$; $R = -0.720$	$P = .0008$; $R = -0.456$
Center, 1 mm	$P < .0001$; $R = -0.701$	$P < .0001$; $R = -0.690$	$P = .0447$; $R = -0.288$
Nasal, 0.5-1.5 mm	$P < .0001$; $R = -0.673$	$P < .0001$; $R = -0.662$	$P = .0185$; $R = -0.334$
Nasal, 1.5-3.0 mm	$P < .0001$; $R = -0.541$	$P = .0002$; $R = -0.505$	$P = .5717$; $R = -0.083$
Retinal thickness, vertical scan			
Inferior, 1.5-3.0 mm	$P < .0001$; $R = -0.551$	$P = .0002$; $R = -0.516$	$P = .0008$; $R = -0.467$
Inferior, 0.5-1.5 mm	$P < .0001$; $R = -0.617$	$P < .0001$; $R = -0.528$	$P = .0030$; $R = -0.419$
Center, 1 mm	$P < .0001$; $R = -0.601$	$P < .0001$; $R = -0.609$	$P = .1477$; $R = -0.215$
Superior, 0.5-1.5 mm	$P < .0001$; $R = -0.633$	$P < .0001$; $R = -0.606$	$P = .0655$; $R = -0.271$
Superior, 1.5-3.0 mm	$P < .0001$; $R = -0.608$	$P < .0001$; $R = -0.640$	$P = .8814$; $R = 0.022$

of structural changes in OCT images of ERM. Results from multiple linear regression analysis showed that parallelism in both the horizontal and vertical scans contributed most to the horizontal and vertical metamorphopsia scores, implying that parallelism correlated with metamorphopsia score better than did retinal thickness.

Parallelism represents the positional relationship among line segments rather than retinal thickness. Although our selection of the parameter parallelism was first based on its potential to evaluate retinal layer integrity using the full thickness of the retina instead of local layer thickness, we challenged our results by also evaluating its usefulness in the inner and outer layers in the current study. As a result, inner-layer parallelism correlated strongly with metamorphopsia score and visual acuity, while outer-layer parallelism had a modest relationship with these visual functions, suggesting that the contribution made by the parallelism of the inner layer to visual function was greater than that made by the outer layer in this study.

A number of studies have reported relationships between retinal morphologic features and metamorphopsia in ERM. Watanabe and associates,[34] Kim and associates,[14] and Okamoto and associates[13] used SDOCT and reported a significant relationship between inner nuclear layer thickness and metamorphopsia. Arimura and associates investigated the relationship between the degree of retinal contraction and the degree of metamorphopsia, and found that there were significant positive correlations between horizontal contraction of the retina and vertical metamorphopsia score and between vertical contraction of the retina and horizontal metamorphopsia score.[35] Collectively, these studies suggest that metamorphopsia in patients with ERM associates with pathologic changes in the inner layer of the retina but not with photoreceptor status. Our results also showed that parallelism of the inner layer correlated strongly with metamorphopsia score. However, Ooto and associates described that eyes with ERM showed abnormal photoreceptor cone mosaic patterns and found that the presence of "microfolds" (a characteristic finding that might correspond to contraction in the photoreceptor layer caused by shrinkage of the ERM) was associated with metamorphopsia by using adaptive-optics scanning laser ophthalmoscopy images, which suggested involvement of the photoreceptor layer in metamorphopsia.[24] In our study, parallelism in the outer layer in both horizontal and vertical scans showed modest correlations with horizontal or vertical metamorphopsia score. Thus, parallelism in the outer layer may have the potential of reflecting the photoreceptor integrity.

A classical digital filtering process was used to generate skeletonized images for calculation of parallelism in this study.[28–30] The benefits of image analysis based on a simple filtering process are its low computational complexity and faithfulness to the original images without segmentation failure. However, as stated before, extraction of structures other than the boundaries of retinal layers, such as vessels and vessel shadows in the vertical scan, might be considered flaws. On the other hand, considering that parallelism can represent changes in the layered structure, parallelism may have the potential to automatically detect abnormal findings in OCT images even in cases with normal retinal thickness. Moreover, parallelism can be used as a parameter of complexity of images, thereby enabling quantification of complicated findings such as retinal structural changes in age-related macular degeneration[9] or hyper-reflective foci,[33,36] cystoid space,[27] microaneurysm,[37] and degenerated photoreceptor layers in diabetic macular edema.[33] Evaluation of parallelism will be tested in retinal diseases other than ERM and using different OCT machines in future.

Our study has the following limitations: (1) sample size was relatively small; and (2) there is room for improvement in the filtering process.

In conclusion, parallelism is proposed as a new robust and practical parameter for structural integrity. This parameter reflects how parallel the layers are to each other in OCT images. Parallelism was significantly lower in eyes with ERM than in normal eyes, and correlated strongly with metamorphopsia and visual acuity in eyes with ERM.

ALL AUTHORS HAVE COMPLETED AND SUBMITTED THE ICMJE FORM FOR DISCLOSURE OF POTENTIAL CONFLICTS OF INTEREST and none were reported. The authors indicate no funding support. Contributions of authors: design of the study (A.U., T.M., K.O., N.Y.); conduct of the study (A.U., T.M., N.U., K.O., K.N., S.Y., Y.D., N.Y.); collection, management, analysis, and interpretation of the data (A.U., T.M., N.U., K.O., K.N., S.Y., Y.D., N.Y.); preparation, review, or approval of the manuscript (A.U., T.M., N.U., K.O., K.N., S.Y., Y.D., N.Y.).

REFERENCES

1. Huang D, Swanson EA, Lin CP, et al. Optical coherence tomography. *Science* 1991;254(5035):1178–1181.
2. Stopa M, Bower BA, Davies E, Izatt JA, Toth CA. Correlation of pathologic features in spectral domain optical coherence tomography with conventional retinal studies. *Retina* 2008;28(2):298–308.
3. Koizumi H, Spaide RF, Fisher YL, Freund KB, Klancnik JM Jr, Yannuzzi LA. Three-dimensional evaluation of vitreomacular traction and epiretinal membrane using spectral-domain optical coherence tomography. *Am J Ophthalmol* 2008; 145(3):509–517.
4. Georgopoulos M, Geitzenauer W, Ahlers C, Simader C, Scholda C, Schmidt-Erfurth U. [High-resolution optical coherence tomography to evaluate vitreomacular traction before and after membrane peeling]. *Ophthalmologe* 2008; 105(8):753–760.
5. Hee MR, Puliafito CA, Wong C, et al. Quantitative assessment of macular edema with optical coherence tomography. *Arch Ophthalmol* 1995;113(8):1019–1029.
6. Parravano M, Oddone F, Boccassini B, et al. Reproducibility of macular thickness measurements using Cirrus SD-OCT in neovascular age-related macular degeneration. *Invest Ophthalmol Vis Sci* 2010;51(9):4788–4791.
7. Kiernan DF, Mieler WF, Hariprasad SM. Spectral-domain optical coherence tomography: a comparison of modern high-resolution retinal imaging systems. *Am J Ophthalmol* 2010;149(1):18–31.
8. Sakamoto A, Hangai M, Yoshimura N. Spectral-domain optical coherence tomography with multiple B-scan averaging for enhanced imaging of retinal diseases. *Ophthalmology* 2008;115(6):1071–1078.e1077.
9. Fleckenstein M, Charbel Issa P, Helb HM, et al. High-resolution spectral domain-OCT imaging in geographic atrophy associated with age-related macular degeneration. *Invest Ophthalmol Vis Sci* 2008;49(9):4137–4144.
10. Yamaike N, Tsujikawa A, Ota M, et al. Three-dimensional imaging of cystoid macular edema in retinal vein occlusion. *Ophthalmology* 2008;115(2):355–362.e352.
11. Forooghian F, Stetson PF, Meyer SA, et al. Relationship between photoreceptor outer segment length and visual acuity in diabetic macular edema. *Retina* 2010;30(1):63–70.
12. Inoue M, Morita S, Watanabe Y, et al. Inner segment/outer segment junction assessed by spectral-domain optical coherence tomography in patients with idiopathic epiretinal membrane. *Am J Ophthalmol* 2010;150(6):834–839.
13. Okamoto F, Sugiura Y, Okamoto Y, Hiraoka T, Oshika T. Associations between metamorphopsia and foveal microstructure in patients with epiretinal membrane. *Invest Ophthalmol Vis Sci* 2012;53(11):6770–6775.
14. Kim JH, Kang SW, Kong MG, Ha HS. Assessment of retinal layers and visual rehabilitation after epiretinal membrane removal. *Graefes Arch Clin Exp Ophthalmol* 2013;251(4): 1055–1064.
15. Nukada M, Hangai M, Mori S, et al. Detection of localized retinal nerve fiber layer defects in glaucoma using enhanced spectral-domain optical coherence tomography. *Ophthalmology* 2011;118(6):1038–1048.
16. Morooka S, Hangai M, Nukada M, et al. Wide 3-dimensional macular ganglion cell complex imaging with spectral-domain optical coherence tomography in glaucoma. *Invest Ophthalmol Vis Sci* 2012;53(8):4805–4812.
17. Hirashima T, Hangai M, Nukada M, et al. Frequency-doubling technology and retinal measurements with spectral-domain optical coherence tomography in preperimetric glaucoma. *Graefes Arch Clin Exp Ophthalmol* 2013; 251(1):129–137.
18. Murakami T, Nishijima K, Akagi T, et al. Segmentational analysis of retinal thickness after vitrectomy in diabetic macular edema. *Invest Ophthalmol Vis Sci* 2012;53(10):6668–6674.
19. Krebs I, Hagen S, Smretschnig E, Womastek I, Brannath W, Binder S. Reproducibility of segmentation error correction in age-related macular degeneration: Stratus versus Cirrus OCT. *Br J Ophthalmol* 2012;96(2):271–275.
20. Takayama K, Hangai M, Durbin M, et al. A novel method to detect local ganglion cell loss in early glaucoma using spectral-domain optical coherence tomography. *Invest Ophthalmol Vis Sci* 2012;53(11):6904–6913.
21. Wanek J, Zelkha R, Lim JI, Shahidi M. Feasibility of a method for en face imaging of photoreceptor cell integrity. *Am J Ophthalmol* 2011;152(5):807–814.e801.
22. Yang Q, Reisman CA, Chan K, Ramachandran R, Raza A, Hood DC. Automated segmentation of outer retinal layers in macular OCT images of patients with retinitis pigmentosa. *Biomed Opt Express* 2011;2(9):2493–2503.
23. Tilleul J, Querques G, Canoui-Poitrine F, Leveziel N, Souied EH. Assessment of a spectral domain OCT segmentation software in a retrospective cohort study of exudative AMD patients. *Ophthalmologica* 2013;229(2):80–85.
24. Ooto S, Hangai M, Takayama K, et al. High-resolution imaging of the photoreceptor layer in epiretinal membrane using adaptive optics scanning laser ophthalmoscopy. *Ophthalmology* 2011;118(5):873–881.
25. Yoneda A, Higaki T, Kutsuna N, et al. Chemical genetic screening identifies a novel inhibitor of parallel alignment of cortical microtubules and cellulose microfibrils. *Plant Cell Physiol* 2007;48(10):1393–1403.

26. Ueda H, Yokota E, Kutsuna N, et al. Myosin-dependent endoplasmic reticulum motility and F-actin organization in plant cells. *Proc Natl Acad Sci U S A* 2010;107(15):6894–6899.
27. Murakami T, Nishijima K, Sakamoto A, Ota M, Horii T, Yoshimura N. Foveal cystoid spaces are associated with enlarged foveal avascular zone and microaneurysms in diabetic macular edema. *Ophthalmology* 2011;118(2):359–367.
28. Canny J. A computational approach to edge detection. *IEEE Trans Pattern Anal Mach Intell* 1986;8(6):679–698.
29. Deriche R. Using Canny criteria to derive a recursively implemented optimal edge detector. *Int J Comput Vis* 1987;1(2):167–187.
30. Jacob M, Unser M. Design of steerable filters for feature detection using Canny-like criteria. *IEEE Trans Pattern Anal Mach Intell* 2004;26(8):1007–1019.
31. Zhang B, Zhang L, Zhang L, Karray F. Retinal vessel extraction by matched filter with first-order derivative of Gaussian. *Comput Biol Med* 2010;40(4):438–445.
32. Otsu N. A threshold selection method from gray-level histograms. *IEEE Trans Syst Man Cybern* 1979;9(1):62–66.
33. Uji A, Murakami T, Nishijima K, et al. Association between hyperreflective foci in the outer retina, status of photoreceptor layer, and visual acuity in diabetic macular edema. *Am J Ophthalmol* 2012;153(4):710–717, 717.e711.
34. Watanabe A, Arimoto S, Nishi O. Correlation between metamorphopsia and epiretinal membrane optical coherence tomography findings. *Ophthalmology* 2009;116(9):1788–1793.
35. Arimura E, Matsumoto C, Okuyama S, Takada S, Hashimoto S, Shimomura Y. Retinal contraction and metamorphopsia scores in eyes with idiopathic epiretinal membrane. *Invest Ophthalmol Vis Sci* 2005;46(8):2961–2966.
36. Bolz M, Schmidt-Erfurth U, Deak G, Mylonas G, Kriechbaum K, Scholda C. Optical coherence tomographic hyperreflective foci: a morphologic sign of lipid extravasation in diabetic macular edema. *Ophthalmology* 2009;116(5):914–920.
37. Horii T, Murakami T, Nishijima K, Sakamoto A, Ota M, Yoshimura N. Optical coherence tomographic characteristics of microaneurysms in diabetic retinopathy. *Am J Ophthalmol* 2010;150(6):840–848.

Biosketch

Akihito Uji, MD, PhD is an Assistant Professor of Ophthalmology at Kyoto University, Kyoto, Japan. He received his MD and PhD degrees from Okayama University Graduate School of Medicine, Okayama, Japan. His interests are diabetic retinopathy and image analysis studies.

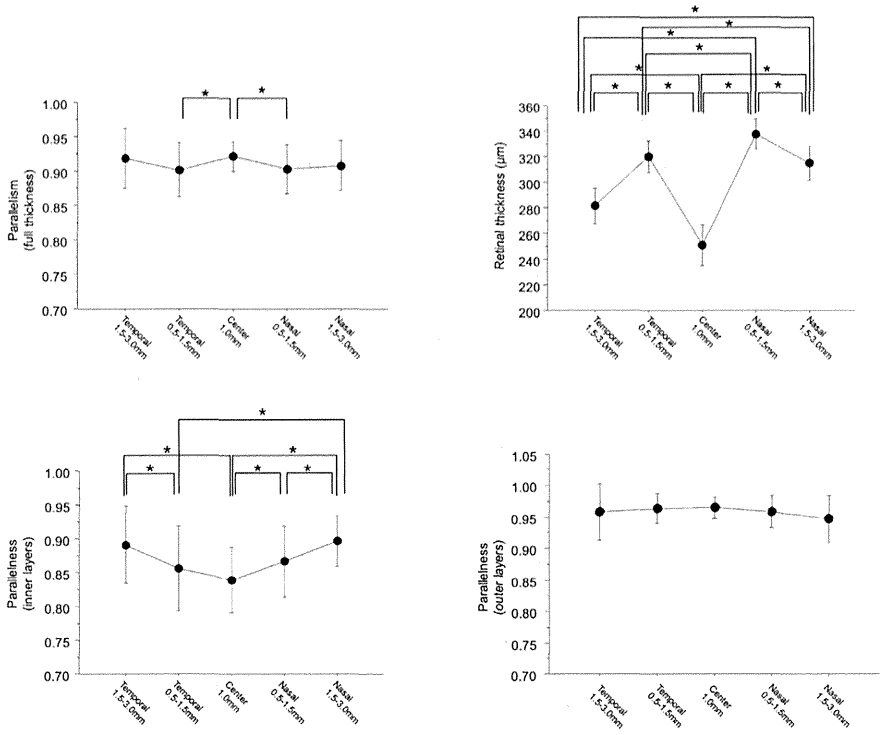

SUPPLEMENTAL FIGURE 1. Parallelism of retinal layers evaluated in horizontal line scan of normal subjects. (Top left) In the horizontal spectral-domain optical coherence tomography scan, significant differences were shown in full-thickness parallelism among 5 subfields (center [1 mm], 2 parafovea [temporal and nasal, 0.5-1.5 mm], and 2 perifovea [temporal and nasal, 1.5-3.0 mm]). (Top right) Retinal thickness was smallest in the center (1 mm) and was largest in the parafovea (0.5-1.5 mm). (Bottom left) Parallelism in the center (1 mm) was significantly smaller than those of the perifovea (1.5-3.0 mm) and parafovea (nasal, 0.5-1.5 mm) in the inner layer. (Bottom right) Significant differences were not shown in outer-layer parallelism among 5 subfields. *$P < .05$, paired t test followed by Bonferroni correction.

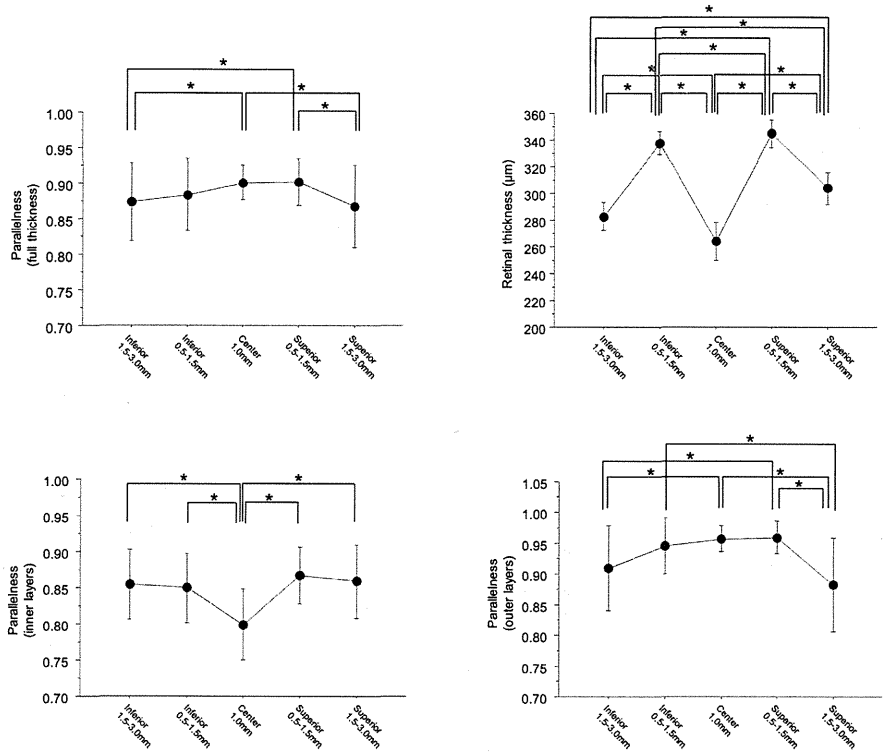

SUPPLEMENTAL FIGURE 2. Parallelism of retinal layers evaluated in vertical line scan of normal subjects. (Top left, Bottom left, Bottom right) In the vertical scan, significant differences were shown in full-thickness, inner-layer, and outer-layer parallelism. Parallelism of the perifovea (1.5-3.0 mm) tended to be smaller than parallelism of the other subfields, and significant differences in full-thickness and outer-layer parallelism were observed between the perifovea and some of the other subfields. Vessel shadows were imaged as lines perpendicular to the retinal layers in vertical scans, which might have caused decreased parallelism in the perifovea. (Top right) Retinal thickness was smallest in the center (1 mm) and was largest in the parafovea (0.5–1.5 mm). *$P < .05$, paired t test followed by Bonferroni correction.

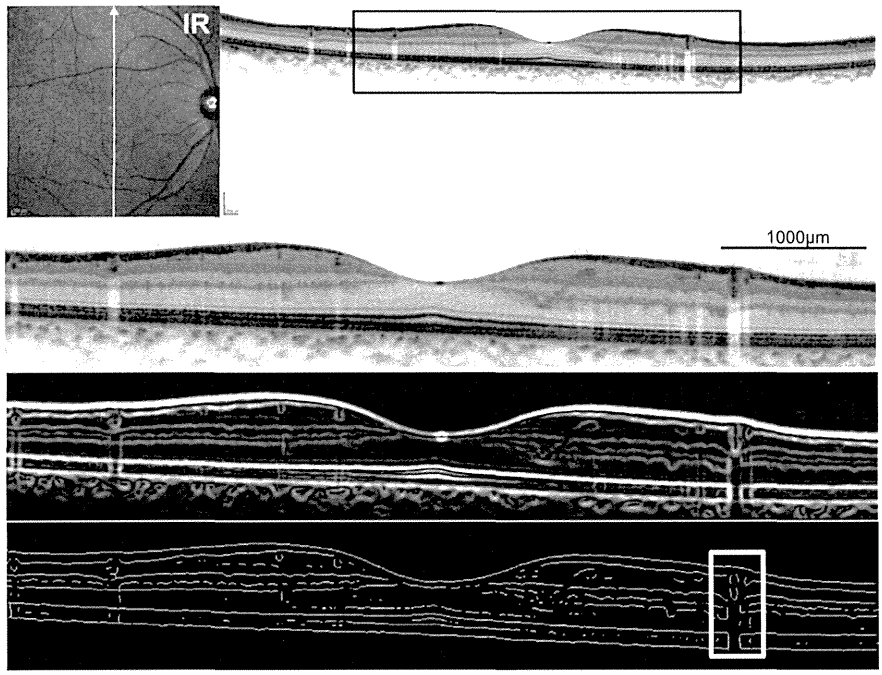

SUPPLEMENTAL FIGURE 3. Extraction of skeletonized image from retinal layers in vertical line scan of optical coherence tomographic images. Images of the right eye of a 65-year-old man from our database of normal volunteers. (Top row) Vertical line scan thorough the fovea of the infrared (IR) spectral-domain optical coherence tomography (SDOCT) image. (Second row) SDOCT image of the 6-mm section outlined in black in top row. (Third row) Filtered image of second row after application of derivative of a Gaussian filter for edge detection. (Bottom row) Skeletonized SDOCT image generated from third row. Note that vessel shadows are imaged as lines perpendicular to the retinal layers (outlined in white), which might have contributed to decreased parallelism in the perifovea (inferior, 1.5-3.0 mm) compared with the horizontal scan. Parallelism calculated for the 6-mm section, full thickness of the center (1 mm), parafovea (superior, 0.5-1.5 mm), and perifovea (superior, 1.5-3.0 mm) was 0.844, 0.928, 0.885, and 0.784, respectively.